follows:

Step 1: calculate and $\sigma_{ETX}(i)$ of path P_i from c through candidate parent $i\,(i=1,2,\cdots,n)$ to the root.

Step 2: arrange $ETX(i)$ values in ascending order, then the paths with the first three minimum $ETX(i)$ values are composed into the alternative path set. If fewer than three, then select all for the alternative path set.

Step 3: the path in the alternative path set with the minimum $\sigma_{ETX}(i)$, will be selected as the optimal path. For example, if $\sigma_{ETX}(f)$ is the minimum value in the alternative path set, then the path P_f (the path from c through candidate parent f to the root) can be selected as the optimal path, and candidate parent f is the preferred parent.

Clearly, comprehensive evaluation of the ETX sum, mean and standard deviation of links in a path not only ensures link quality, but also avoids selection of an optimal path with large ETX links. To facilitate combining ETX with other routing metrics, normalization is required, as shown in Eq. (12). The final ETX routing metric formula used in this paper is shown in Eq. (13).

$$\underset{normalization}{\sigma_{ETX}(i)}=\frac{\sigma_{ETX}(i)}{\sum_{i=1}^{n}\sigma_{ETX}(i)},0\le \underset{normalization}{\sigma_{ETX}(i)}\le 1 \tag{12}$$

$$\psi(i)=\begin{cases}0 & i=root\\ \underset{normalization}{\sigma_{ETX}(i)} & i\neq root\end{cases} \tag{13}$$

(4) Delay (D)

Similar to the ETX calculation rules, the delay sum, mean and standard deviation of links in a path are comprehensively evaluated to avoid selecting an optimal path that encounters one or more large delay links. Suppose that $D(i)$, $\overline{D(i)}$ and $\sigma_D(i)$ are the delay sum, mean and standard deviation of links in the path from c through the candidate parent $i\,(i=1,2,\cdots,n)$ to the root, and can be calculated according to Eq. (14).

$$\begin{aligned}&D(i)=D_1+D_2+,\cdots,+D_{h_i}\\ &\overline{D(i)}=\frac{D_i}{h_i}\\ &\sigma_D(i)=\sqrt{\frac{1}{h_i-1}\sum_{k=1}^{h_i}(D_k-\overline{D}_i)^2}\end{aligned} \tag{14}$$

In Eq. (14), h_i is the hop count of path P_i from node c through candidate parent i to the root. The specific lexical rules of $D(i)$, $\overline{D(i)}$ and $\sigma_D(i)$ are as follows:

Step 1: calculate $D(i)$, $\overline{D(i)}$ and $\sigma_D(i)$ of path P_i from node c through the candidate parent i to the root.

Step 2: arrange $D(i)$ values in ascending order, then the paths with the first three minimum $D(i)$ values are composed into the alternative path set. If fewer than three, then select all of them into the alternative path set.

Step 3: the path in the alternative path set with the minimum $\sigma_D(i)$, will be selected as the optimal path. For example, if $\sigma_D(f)$ is the minimum value in the alternative path set, then the path P_f (the path from c through candidate parent f to the root) can be selected as the optimal path, and the candidate parent f is the preferred parent.

Clearly, comprehensive evaluation of the delay sum, mean and standard deviation of links in a path not only ensures real-time performance, but also avoids selecting an optimal path with large delay links. To facilitate combining delay with other routing metrics, normalization is required, as shown in Eq. (15). The final delay routing metric formula used in this paper is shown in Eq. (16).

$$\underset{normalization}{\sigma_D(i)}=\frac{\sigma_D(i)}{\sum_{i=1}^{n}\sigma_D(i)},0\le \underset{normalization}{\sigma_D(i)}\le 1 \tag{15}$$

$$\xi(i)=\begin{cases}0 & i=root\\ \underset{normalization}{\sigma_D(i)} & i\neq root\end{cases} \tag{16}$$

(5) Hop count

Hop count, the number of hops between a candidate parent and the root, can be used to avoid selecting a candidate parent with a large hop count as the preferred parent. The hop count is evaluated in the process of calculating the ETX and delay standard deviation. Therefore, this paper will not evaluate the hop count routing metric separately.

In summary, CAR-TMO evaluates all the above important routing metrics, resulting in better network performance.

3.4 Novel membership functions of routing metrics

CAR-TMO uses an assignment method to deter-

mine membership functions of routing metrics used in CA-RM. The membership functions are as follows.

(1) REI membership function

CAR-TMO selects an arc-tangent membership function as the REI membership function, as shown in Eq. (17). *REI*(*i*) can be calculated according to Eq. (8). The greater the *REI*(*i*), the greater the probability that the neighbor becomes the preferred parent, and vice versa (Fig. 6).

$$\varphi_1(i)=\begin{cases}0.01 & \alpha<REI(i)<1\\ F(REI(i))-F(\alpha)+0.5 & 0<REI(i)\le\alpha\end{cases}$$
$$F(REI(i))=\frac{1}{\pi}\arctan[\lambda(\alpha\text{-}REI(i))],\ \lambda=25,\ \alpha=0.6 \quad (17)$$

(2) BOR membership function

CAR-TMO selects a Gaussian membership function as the BOR membership function, as shown in Eq. (18). *BOR*(*i*) can be calculated according to Eq. (9). The smaller the *BOR*(*i*), the greater the probability that the neighbor becomes the preferred parent, and vice versa (Fig. 6).

$$\varphi_2(i)=\exp(-\frac{(BOR(i)-c)^2}{2\sigma^2}),\ c=0,\ \sigma^2=0.0625 \quad (18)$$

(3) ETX membership function

CAR-TMO selects a descending semi-normal distribution membership function as the ETX membership function, as shown in Eq. (19). $\psi(i)$ can be calculated according to Eq. (13). The smaller the $\psi(i)$, the greater the probability that the neighbor becomes the preferred parent, and vice versa (Fig. 6).

$$\varphi_3(i)=\exp(-k(\psi(i)-a)^2),\ k=15,\ a=0.01 \quad (19)$$

(4) Delay membership function

CAR-TMO selects a Gaussian membership function as the delay membership function, as shown in Eq. (20). $\xi(i)$ can be calculated according to Eq. (16). The smaller the $\xi(i)$, the smaller the probability that the neighbor becomes the preferred parent, and vice versa (Fig. 6).

$$\varphi_4(i)=\exp(-\frac{(\xi(i)-c)^2}{2\sigma^2}),\ c=0,\ \sigma^2=\frac{1}{30} \quad (20)$$

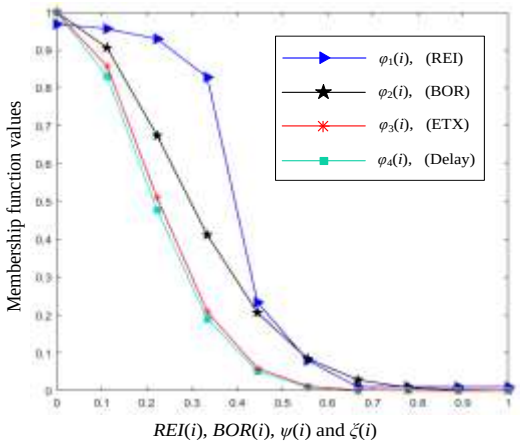

Fig. 6: Membership function curve

3.5 Novel comprehensive membership function

According to the triangle module operator, CAR-TMO fuses the membership function of each routing metric designed above into a comprehensive membership function. As shown in Eq. (21), CAR-TMO designs a four-dimensional triangle module operator. It conforms to the definition of a triangle module operator and can be used to fuse the membership functions of routing metrics to evaluate candidate parents comprehensively.

$$f[\varphi_1(i),\varphi_2(i),\varphi_3(i),\varphi_4(i)]=\frac{\prod_{j=1}^{4}\varphi_j(i)}{\prod_{j=1}^{4}\varphi_j(i)+\prod_{j=1}^{4}(1-\varphi_j(i))} \quad (21)$$

In Eq. (21), $\varphi_j(i)$ $(i=1,2,\cdots,n;\ j=1,2,3,4)$ is the membership function of the *j*-th routing metric of the *i*-th candidate parent. Eq. (21) has the following characteristics:

(1) Shrinking dimension mapping:

f:[0, 1]^4→[0, 1];

(2) $f[\varphi_1(i),\varphi_2(i),\varphi_3(i),\varphi_4(i)]=0$, if $\varphi_j(i)=0$; $f[\varphi_1(i),\varphi_2(i),\varphi_3(i),\varphi_4(i)]=1$, if $\varphi_j(i)=1$;

(3) $f[\varphi_1(i),\varphi_2(i),\varphi_3(i),\varphi_4(i)]\le f[\varphi_1(i'),\varphi_2(i'),\varphi_3(i'),\varphi_4(i')]$,if $\varphi_j(i)\le\varphi_j(i')$;

(4) $f[\varphi_1(i),\varphi_2(i),\varphi_3(i),\varphi_4(i)]=f[\varphi_2(i),\varphi_1(i),\varphi_3(i),\varphi_4(i)]=f[\varphi_3(i),\varphi_2(i),\varphi_1(i),\varphi_4(i)]=\cdots$;

(5) Strengthening similar information:

$f[\varphi_1(i),\varphi_2(i),\varphi_3(i),\varphi_4(i)] \geq \max(\varphi_1(i),\varphi_2(i),\varphi_3(i),\varphi_4(i))$, if $\varphi_j(i) \geq 0.5$;

$f[\varphi_1(i),\varphi_2(i),\varphi_3(i),\varphi_4(i)] \leq \min(\varphi_1(i),\varphi_2(i),\varphi_3(i),\varphi_4(i))$, if $\varphi_j(i) \leq 0.5$;

(6) Reconciling contradictory information:

$\min(\varphi_1(i),\varphi_2(i),\varphi_3(i),\varphi_4(i)) \leq f[\varphi_1(i),\varphi_2(i),\varphi_3(i),\varphi_4(i)] \leq \max(\varphi_1(i),\varphi_2(i),\varphi_3(i),\varphi_4(i))$, if $\min(\varphi_1(i),\varphi_2(i),\varphi_3(i),\varphi_4(i)) < 0.5 < \max(\varphi_1(i),\varphi_2(i),\varphi_3(i),\varphi_4(i))$.

Among them, $\varphi_j(i), \varphi_j(i') \in [0,1]$, $j = 1,2,3,4$.

Through the triangle module operator, the selection probabilities of preponderant nodes can be enhanced and those of poor nodes can be weakened. Meanwhile, contradictions appearing in REI, BOR, ETX and Delay among candidate parents can also be reconciled and balance the selection criteria of the preferred parent. For instance, if REI, BOR, ETX and Delay of a candidate parent are all favourable (their membership function values are all greater than 0.5), the probability of selecting this candidate parent as preferred parent will increase, and vice versa. If there are contradictions between REI, BOR, ETX and Delay of a candidate parent (several of their membership function values are greater than 0.5 and several are less than 0.5), the probability of selecting this candidate parent as the preferred parent is determined by their neutral value. Therefore, through the triangle module operator, CAR-TMO can comprehensively evaluate routing metrics in different aspects of candidate parents. Then the optimal preferred parent can be selected and network performance improved effectively.

3.6 Context Aware objective function (CA-OF)

According to the comprehensive membership function (Eq. (21)) and the maximum membership principle, the novel comprehensive context aware objective function (CA-OF) can be designed as shown in Eq. (23).

$$OF_{CA}(i) = \frac{1}{f[\varphi_1(i),\varphi_2(i),\varphi_3(i),\varphi_4(i)]+1}, i = 1,2,\cdots,n \quad (22)$$

$$OF_{CA} = \min(OF_{CA}(i)), i = 1,2,\cdots,n \quad (23)$$

The objective function is the basis for obtaining and updating routing metric information, calculating node rank value, constructing network topology and selecting the optimal route. The new proposed CA-OF can comprehensively evaluate REI, BOR, ETX, and Delay of candidate parents through the triangle module operator and the maximum membership principle. Then the node rank value, network topology and optimal route can be calculated optimally.

3.7 Novel Rank calculation method

The rank of a node represents its position relative to the root. To avoid loops, the rank value should strictly increase in the Down direction (from the root towards the leaf nodes) and decrease in the Up direction (from the leaf nodes to the root). It can be calculated according to objective function. Therefore, based on CA-OF, a novel rank calculation method is proposed.

Firstly, the rank of the root is set as 1.0. Then the rank of other non-root nodes such as *c* can be calculated according to Eq. (24). $R_c(i)$ is the rank of *c*, which is based on the route from *c* through candidate parent *i* to the root. $R_{cp}(i)$, advertised by *i* through DIO, is the rank of *i*. $(OF_{CA}(i)+1)$ is the calculated CA-OF value of the link from *c* to candidate parent *i*.

$$R_c(i) = R_{cp}(i) + (OF_{CA}(i)+1), i = 1,2,\cdots,n \quad (24)$$

According to Eq. (24), $\{R_c(1), R_c(2),\cdots, R_c(n)\}$ can be obtained. If $\min\{R_c(1), R_c(2),\cdots, R_c(n)\}=R_c(f)$, then the candidate parent *f* can be selected as the preferred parent.

3.8 Novel preferred parent selection mechanisms

From section 3.7, it can be seen that through *n* candidate parents, *c* can obtain *n* rank values $\{R_c(1), R_c(2),\cdots, R_c(n)\}$. If $\min\{R_c(1), R_c(2),\cdots, R_c(n)\} = R_c(f)$, then *f* will be selected as the preferred parent. However, this preferred parent selection method is not applicable to all cases, such as when there are two or more equal and minimum rank values. Therefore, CAR-TMO proposes novel preferred parent selecting mechanisms, as follows:

(1) If the rank calculated by *c* through its current preferred parent is greater than that calculated through a candidate parent, but the difference between the two is less than the threshold of the preferred parent replacement, then the current preferred parent will not be replaced. In this way, the stability of the network topology is guaranteed as well as the network performance.

(2) If the rank calculated by *c* through its current preferred parent is the minimum, and equal to the rank calculated by *c* through several other candidate parents, then to guarantee stability of the network topology, the current preferred parent will not be replaced.

(3) If the rank calculated by *c* through a candidate parent is less than 1.0 or greater than 1000 (the node number in LLN), then this candidate parent must be eliminated from the candidate parent set. Because the quality of this candidate parent is too poor to deliver any packets or the rank calculated through this candidate parent is incorrect, it needs to recalculate or become a leaf.

(4) When selecting the preferred parent, if there are two or more equal and minimum rank values, then the candidate parent with the largest candidate parent set will be selected as the preferred parent. The larger the candidate parent set, the larger the selection range of the preferred parent. Therefore, the more likely it is to select the optimal node as the preferred parent.

(5) If *c* has only one candidate parent, then *c* waits for a period of time to obtain more candidate parents. After that, if *c* has two or more candidate parents, *c* selects its preferred parent through CAR-TMO. Otherwise, *c* directly chooses this candidate parent as its preferred parent without executing CAR-TMO, and the rank of *c* equals the rank of this candidate parent plus 1.

3.9 Computational complexity analysis

The computational complexity of CAR-TMO and several RPL improvements can be represented as $O(N.H)$. N is the number of candidate parents and H is the number of hops. The computational complexity of the RPL algorithms increases with increasing network size. However, CAR-TMO does not increase computational complexity compared to these existing algorithms.

4 Performance evaluation

To quantitatively evaluate and compare the new proposed CAR-TMO algorithm and several popular improvements of RPL, such as ETXOF (in MRHOF manner), OF0, and 0.8ETX+0.2REI, we carried out a series of experiments using OPNET14.5.

4.1 Statistic metrics

We selected six important statistic metrics (Table 4) to comprehensively evaluate and compare the performance of CAR-TMO and several popular improvements of RPL.

To improve the accuracy of the experimental results without loss of generality, the average values from many simulations were taken as the final result.

4.2 Simulation parameters

Nodes were randomly deployed in a 500m×500m network area. The arrival of packets conformed to a Poisson distribution. The initial energy of the nodes was a random value between 0.5J and 15J. If the residual energy of a node was less than 5% of its initial energy, the node was considered dead. Other key parameters used in CAR-TMO are listed in Table 5.

In Table 5, $E(v, d)$ (Nayak and Devulapalli, 2016) can be computed as follows:

$$E(v,d)=\begin{cases}2E_{elec}\times v+\varepsilon_{amp}\times v\times d^2 & d<d_0\\ 2E_{elec}\times v+\varepsilon_{fs}\times v\times d^4 & d>d_0\end{cases} \tag{25}$$

The parameters used in Eq. (25) are explained in Table 6.

Table 4: Statistic metrics

Statistic metrics	Explanations	Formula
Packet delivery ratio (PDR)	The ratio of the number of packets successfully received and total number of packets sent.	$PDR(\%)=\frac{no.\ of\ received\ packts}{no.\ of\ sent\ packts}$
Network latency	Average time required for a packet to reach its destination.	$Latency=\frac{\sum(receive_{time}-send_{time})}{no.\ of\ received\ packets}$
Energy efficiency	Tested by node average residual energy or	

	number of live nodes.	
Hop count	Average hops from source to destination.	$Hop = \sum hops / no.\ of\ nodes$.
Preferred parent changes (PPC)	Average number of preferred parent changes.	$PPC = \sum no.\ of\ ppc / no.\ of\ nodes$.
Control overhead (CO)	Tested by the average number of control messages needed to be transmitted per second.	$CO = \frac{\sum DIO + \sum DIS + \sum DAO}{network\ running\ time}$

Table 5: Simulation parameters

Parameter	Value
Simulation scenario (m2)	500×500
Number of nodes	20, 40, 80, 100
Simulation time (s)	1800
Traffic arrival rate (packet/s)	10
Initial energy (J)	0.5-15
Energy consumption of relaying v bit message	E(v,d)
Packet format	IPv6
Physical and data link layer	IEEE 802.15.4g
Size of packet (bits)	1024
Maximum buffer size (packet number)	16
Minimum buffer size (packet number)	0
Queue type	FIFO
Transmission range (m)	50

Table 6: Parameters used in $E(v, d)$

Parameter	Explanation	Value
E_{elec}	Energy consumption of relaying a 1-bit message.	50 nJ/bit
ε_{amp}	Energy consumption of transmission amplifier sending 1bit message ($d<d_0$).	10 pJ/bit/m^2
ε_{fs}	Energy consumption of transmission amplifier sending 1bit message ($d>d_0$).	0.0013 pJ/bit/m^4
d_0	The threshold	87 m
d	Communication distance between nodes	

4.3 Results and analysis

(1) Average packet delivery ratio (PDR)

Fig. 7 shows the average packet delivery ratio (PDR) of CAR-TMO, ETXOF, OF0, and 0.8ETX+0.2REI. In the initial network operation stage, the PDR of each algorithm is unstable. It gradually reaches a stable state after 1000 s. The PDR of CAR-TMO is obviously higher than that of ETXOF, OF0, and 0.8ETX+0.2REI. This is because CAR-TMO evaluates REI and BOR recursively, and evaluates the sum, mean and standard deviation of ETX and Delay comprehensively. Then, CAR-TMO uses the triangle module operator and maximum membership principle to fuse the context aware composite routing metrics, and constructs the context aware objective function. Therefore, CAR-TMO can comprehensively evaluate routing metrics in different aspects of candidate parents, and select the optimal route to transmit packets. So the PDR of CAR-TMO is significantly higher than that of the other algorithms.

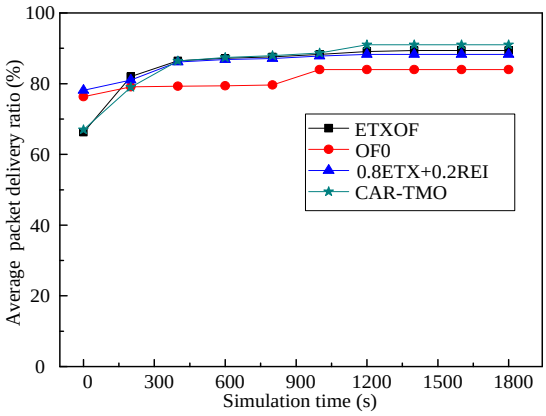

Fig. 7: Average packet delivery ratio

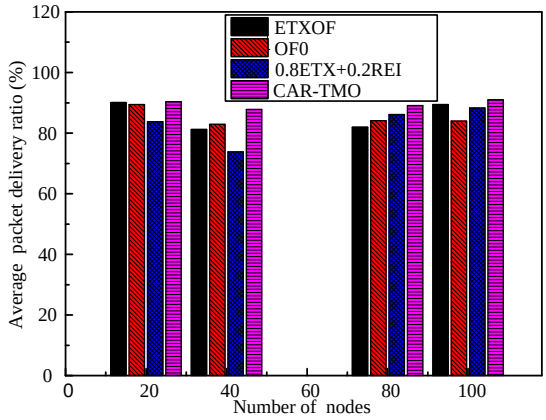

Fig. 8: Average packet delivery ratio in different node number.

The PDR of CAR-TMO, ETXOF, OF0, and 0.8ETX+0.2REI with different numbers of nodes is shown in Fig. 8. The average PDR of CAR-TMO is much higher than that of ETXOF, OF0, and 0.8ETX+0.2REI at different node densities.

(2) Average network latency

Fig. 9 illustrates the average network latency of CAR-TMO, ETXOF, OF0, and 0.8ETX+0.2REI. The network latency of CAR-TMO is notably lower than that of the other algorithms. CAR-TMO improves the path delay calculation method and comprehensively evaluates the sum, mean and standard deviation of Delay. Then the triangle module operator and the maximum membership principle are used. Thereby, CAR-TMO can clearly improve the network latency performance.

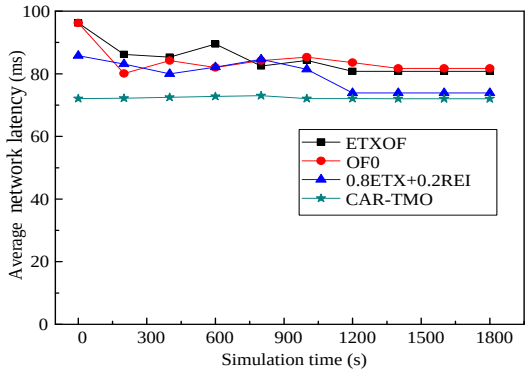

Fig. 9: Average network latency

Fig. 10 shows the average network latency of CAR-TMO, ETXOF, OF0, and 0.8ETX+0.2REI for different numbers of nodes. The average network latency of CAR-TMO is clearly much lower than that of other algorithms at different node densities.

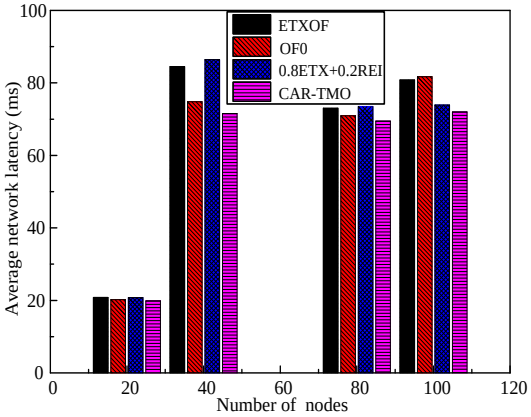

Fig. 10: Average network latency in different node number

(3) Energy efficiency

The average remaining energy and average live node number can represent energy efficiency effectively. Figs. 11 and 12 show these two statistic metrics of CAR-TMO, ETXOF, OF0, and 0.8ETX+0.2REI. The average remaining energy and average live node number of CAR-TMO are much higher than those of ETXOF, OF0, and 0.8ETX+0.2REI. CAR-TMO comprehensively evaluates REI, BOR, ETX and Delay of a candidate parent, proposes the triangle module operator and maximum membership function to construct a context aware objective function, and designs a preferred parent selection mechanism to notably improve energy efficiency.

Fig. 13 shows the average live node number of CAR-TMO, ETXOF, OF0, and 0.8ETX+0.2REI for different numbers of nodes. The average live node number of CAR-TMO is much higher than that of

other algorithms at different node densities.

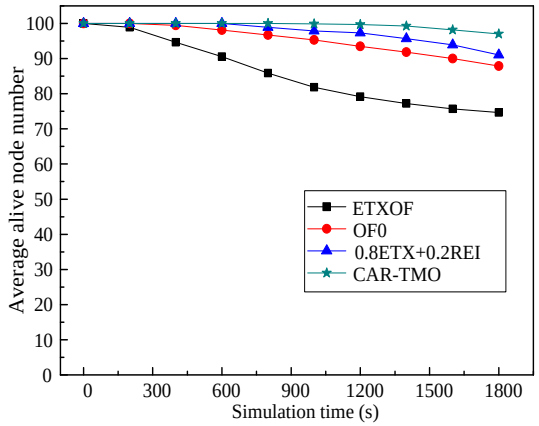

Fig. 11: Average live node number

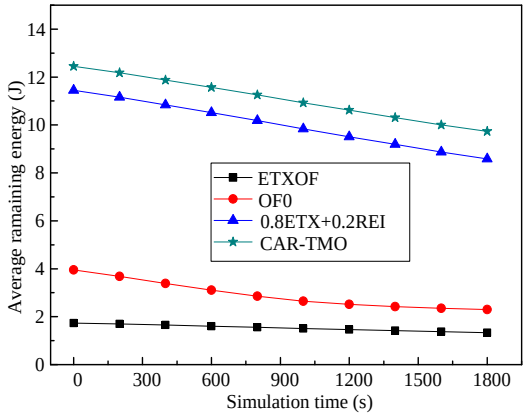

Fig. 12: Average remaining energy

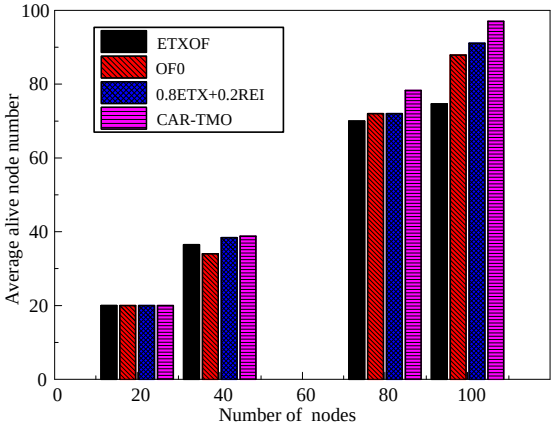

Fig. 13: Average live node number in different node number

(4) Average hop count

The average hop counts of CAR-TMO, ETXOF, OF0, and 0.8ETX+0.2REI are shown in Fig. 14. The hop counts of OF0 and CAR-TMO are lower than those of ETXOF and 0.8ETX+0.2REI. Because OF0 selects the next hop based only on the hop metric, the candidate parent with the lowest hop will be selected as the preferred parent. CAR-TMO fuses hop count, ETX and Delay routing metric, and evaluates them using the triangle module operator and maximum membership principle. Therefore, the average hop counts of CAR-TMO and OF0 are significantly lower than those of ETXOF and 0.8ETX+0.2REI.

The average hop counts of CAR-TMO, ETXOF, OF0, and 0.8ETX+0.2REI for different numbers of nodes is shown in Fig. 15. The average hop count of CAR-TMO is much lower than that of the other algorithms at different node densities.

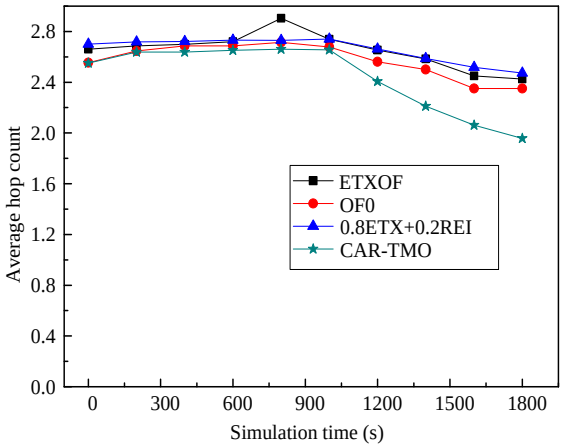

Fig. 14: Average hop count

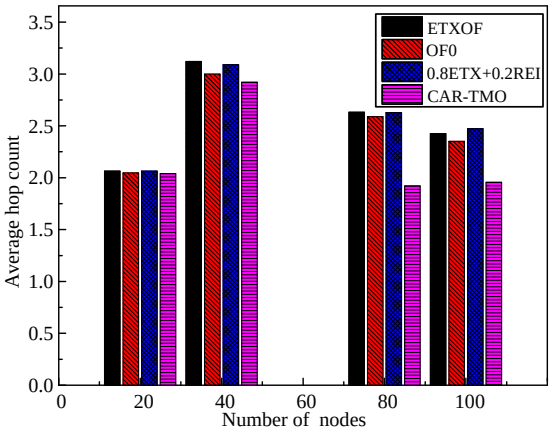

Fig. 15: Average hop count in different node number

(5) Average number of preferred parent changes (PPC)

The average number of preferred parent changes (PPC) reflects the stability of the network topology, and can be used to reconcile network performance and network topology stability. Fig. 16 shows the average number of PPC of CAR-TMO, ETXOF, OF0,

and 0.8ETX+0.2REI. In the initial network operation stage, network topology is constructed, so the PPC number is relatively high. When network topology gradually reaches a stable state after 1000 s, the PPC in CAR-TMO is much lower than that of ETXOF, OF0, and 0.8ETX+0.2REI. Therefore, CAR-TMO can guarantee network topology stability as well as improve network performance effectively.

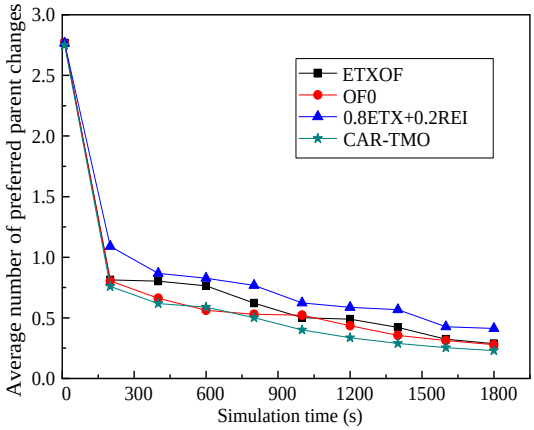

Fig. 16: Average number of preferred parent changes

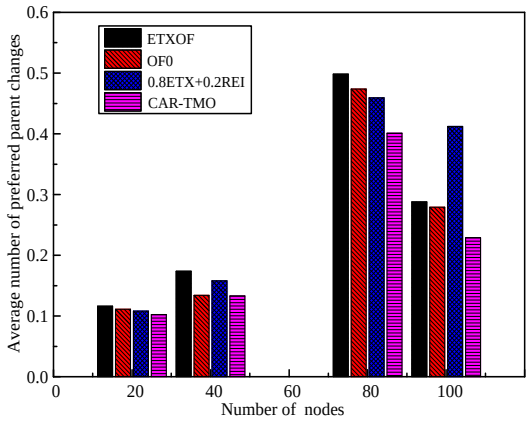

Fig. 17: Average number of preferred parent changes in different node number

Fig. 17 shows the average live node number of CAR-TMO, ETXOF, OF0, and 0.8ETX+0.2REI for different numbers of nodes. The average live node number of CAR-TMO is much higher than that of the other algorithms at different node densities.

(6) Control Overhead (CO)

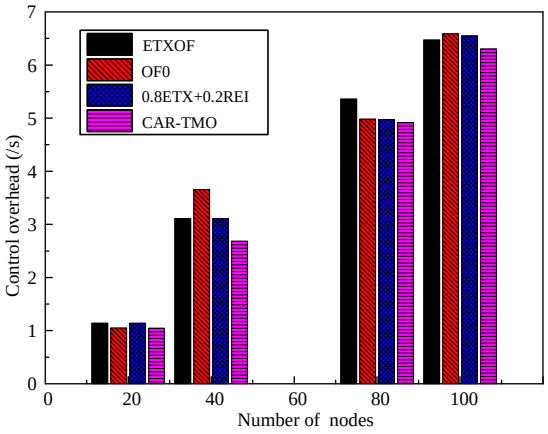

Fig. 18: Control overhead in different node number

The control overhead of CAR-TMO, ETXOF, OF0, and 0.8ETX+0.2REI for different numbers of nodes is shown in Fig. 18. The control overhead of CAR-TMO is much lower than that of ETXOF, OF0, and 0.8ETX+0.2REI at different node densities.

5 Conclusions

In this paper, we propose a novel Context Aware RPL algorithm based on a Triangle Module Operator (CAR-TMO). It designs a novel composite context aware routing metric (CA-RM), novel membership functions of routing metrics, a comprehensive membership function, a new comprehensive context aware objective function, novel rank calculation mechanisms and novel preferred parent (the next hop) selection mechanisms. Through these new designed mechanisms, CAR-TMO can significantly improve network performance as well as guarantee the stability of network topology.

In future work, we will combine 5G or other technologies with RPL to improve the use of LLNs.

Contributors

Yanan CAO designed the research. Yanan CAO and Hao YUAN processed the data. Yanan CAO drafted the manuscript. Hao YUAN helped organize the manuscript. Yanan CAO and Hao YUAN revised and finalized the paper.

Compliance with ethics guidelines

Yanan CAO and Hao YUAN declare that they have no conflict of interest.

References

Ali S, Ali G, 2020. A lightweight load balancing and route

minimizing solution for routing protocol for low-power and lossy networks. *J Computer Networks*, 179. https://doi.org/10.1016/j.comnet.2020.107368

Muhammad MM, Mohammed B, Luca R, 2020. On Providing Differentiated Service Exploiting Multi-Instance RPL for Industrial Low-Power and Lossy Networks. J Wireless Communications and Mobile Computing, 2020. https://doi.org/10.1155/2020/2896561

Memon RA, Li JP, Ahmed J, et al., 2020. Cloud-based vs. blockchain-based IoT: a comparative survey and way forward. J Front Inform Technol Electron Eng 21, 563–586. https://doi.org/10.1631/FITEE.1800343.

Pereira H, Moritz GL, Souza RD, et al., 2020. Increased Network Lifetime and Load Balancing based on Network Interface Average Power Metric for RPL. J IEEE Access, 8: 48686-48696. https://doi.org/10.1109/ACCESS.2020.2979834

Winter T, Thubert P, Brandt A, et al., 2012. RPL: IPv6 Routing Protocol for Low-Power and Lossy Networks. Internet Engineering Task Force (IETF) RFC6550.

Ganesh DR, Patil KK, Suresh L, 2019. Q-FRPML: QoS-Centric Fault-Resilient Routing Protocol for Mobile-WSN Based Low Power Lossy Networks. J Wireless Personal Communications, 105(1): 267-292. https://doi.org/10.1007/s11277-018-6112-8

Thubert P, 2012. Objective function zero for the routing protocol for low-power and lossy networks (RPL). Internet Engineering Task Force (IETF) RFC6552.

Gnawali O, Levis P, 2012. The minimum rank with hysteresis objective function. Internet Engineering Task Force (IETF) RFC 6719.

Wadhaj I, Ghaleb B, Thomson C, et al., 2020. Mitigation Mechanisms Against the DAO Attack on the Routing Protocol for Low Power and Lossy Networks (RPL). J IEEE Access, 8: 43665-43675. https://doi.org/10.1109/ACCESS.2020.2977476

Taghizadeh S, Bobarshad H, Elbiaze H, 2018. CLRPL: context-aware and load balancing RPL for Iot networks under heavy and highly dynamic load. J IEEE Access, 6: 23277-23291. https://doi.org/10.1109/ACCESS.2018.2817128

Alishahi M, Moghaddam MHY, Pourreza HR, 2018. Multi-class routing protocol using virtualization and SDN-enabled architecture for smart grid. J Peer-to-Peer Networking and Applications, 11(3): 380-396. https://doi.org/10.1007/s12083-016-0537-1

Lamaazi H, Benamar N, 2018. OF-EC: A novel energy consumption aware objective function for RPL based on fuzzy logic. J Journal of Network and Computer Applications, 117: 42-58. https://doi.org/10.1016/j.jnca.2018.05.015

Gao L, Zheng Z, Huo M, 2018. Improvement of RPL Protocol Algorithm for Smart Grid. IEEE 18th International Conference on Communication Technology (ICCT), p.927-930. https://doi.org/10.1109/ICCT.2018.8600162

Bhandari K, Hosen A, Cho G, 2018. CoAR: Congestion-Aware Routing Protocol for Low Power and Lossy Networks for IoT Applications[J]. Sensors, 18(11): 3838. https://doi.org/10.3390/s18113838

Al-Kashoash HAA, Al-Nidawi Y, Kemp AH, 2016. Congestion-aware RPL for 6L0WPAN networks. Wireless Telecommunications Symposium (WTS), p.1-6. https://doi.org/10.1109/WTS.2016.7482026

Kim HS, Kim H, Paek J, et al., 2016. Load balancing under heavy traffic in RPL routing protocol for low power and lossy networks. J IEEE Transactions on Mobile Computing, 16(4): 964-979. https://doi.org/10.1109/TMC.2016.2585107

Nassar J, Berthomé M, Dubrulle J, et al., 2018. Multiple Instances QoS Routing in RPL: Application to Smart Grids. J Sensors, 18(8): 2472. https://doi.org/10.3390/s18082472

Kheaksong A, Srisomboon K, Prayote A, et al., 2018. Multicriteria Parent Selection Using Cognitive Radio for RPL in Smart Grid Network. J Wireless Communications and Mobile Computing, 2018. https://doi.org/10.1155/2018/9590576

Araújo H, Rodrigues J, Rabelo R, et al., 2018. A Proposal for IoT Dynamic Routes Selection Based on Contextual Information. J Sensors, 18(2): 353. https://doi.org/10.3390/s18020353

Sanmartin P, Rojas A, Fernandez L, et al. Sigma Routing Metric for RPL Protocol. J Sensors, 2018, 18(4): 1277. https://doi.org/10.3390/s18041277

Sharwari S. Solapure, Harish H, 2020. Kenchannavar. Design and analysis of RPL objective functions using variant routing metrics for IoT applications. J Wireless Networks, 26(6): 4637-4656. https://doi.org/10.1007/s11276-020-02348-6

Trakadas P, Zahariadis T, 2012. Design Guidelines for Routing Metrics Composition in LLN. Internet Engineering Task Force (IETF) draft.

Hassan A, Alshomrani S, Altalhi A, et al., 2016. Improved routing metrics for energy constrained interconnected devices in low-power and lossy networks. J Journal of Communications and Networks, 18(3): 327-332. https://doi.org/10.1109/JCN.2016.000048

Velivasaki THN, Karkazis P, Zahariadis TV, et al., 2014. Trust-aware and link-reliable routing metric composition for wireless sensor networks. J Transactions on Emerging Telecommunications Technologies, 25(5): 539-554. https://doi.org/10.1002/ett.2592

Karkazis P, Trakadas P, Leligou HC, et al., 2013. Evaluating routing metric composition approaches for QoS differentiation in low power and lossy networks. J Wireless networks, 19(6): 1269-1284. https://doi.org/10.1007/s11276-012-0532-2

Miloš N, Milica Š, Dragana M, et al., 2020. Bee Colony Optimization metaheuristic for fuzzy membership functions tuning. J Expert Systems With Applications, 158.

https://doi.org/10.1016/j.eswa.2020.113601

Huynh TT, Lin CM, Le TL, et al., 2020. A New Self-Organizing Fuzzy Cerebellar Model Articulation Controller for Uncertain Nonlinear Systems Using Overlapped Gaussian Membership Functions. J IEEE Transactions on Industrial Electronics, 67(11): 9671-9682.
https://doi.org/10.1109/TIE.2019.2952790

Cao YN, Wu MQ, 2018. RPL Based on Triangle Module Operator for AMI Networks. J China communication, 15(5): 162-172.
https://doi.org/10.1109/CC.2018.8387995

Nayak P, Devulapalli A, 2016. A Fuzzy Logic-Based Clustering Algorithm for WSN to Extend the Network Lifetime. J IEEE Sensors Journal, 16(1): 137-144.
https://doi.org/10.1109/JSEN.2015.2472970